

Comprehensive Analysis of Bifunctional 2DEG-HBTs

T. USAGAWA, P.D. RABINZOHN*, H. MIZUTA, K. HIRUMA, M. KAWATA, and K. YAMAGUCHI

Central Research Laboratory, Hitachi Ltd.,
Kokubunji, Tokyo 185, Japan.

*From Philips Research Organization

L.E.P., 3 Avenue Descartes, Limeil-Brevannes, France.

present address: Matra MHS (Wafer Fab.), La Chantrerie-Route
de Gacher, CP 3008 , 44087 Nantes-Cedex 03, France.

The Bipolar/FET characteristics of the 2DEG-HBT is extensively analyzed by using the two-dimensional numerical simulator based on a drift-diffusion model. For the emitter size of $1 \times 10 \mu\text{m}^2$, the undoped collector thickness of 150 nm, and the collector current density J_c (10^5 A/cm^2), the high cutoff frequency f_T (88 GHz) and the current gain h_{FE} (760) are demonstrated. Moreover, the burried SiO_2 structure for reducing the extrinsic base-collector capacitance C_{bc}^{EXT} shows the extremely high cutoff frequency f_T (160 GHz) and maximum oscillation frequency f_{max} (103 GHz) for the bipolar mode. The optimization of the epitaxial layer structures shows the tradeoffs for the design of a better performance FET (e.g. $G_m = 235 \text{ mS/mm}$ and $f_T = 19 \text{ GHz}$) without sacrificing the bipolar function.

I. Introduction

The 2DEG-HBT (Two-Dimensional Electron Gas Base Heterojunction Bipolar Transistor) [1] is a new functional device, a 'bitransistor', operating as both a bipolar transistor and a FET. The 2DEG at the AlGaAs/GaAs heterointerface acts as either the base of a Pnp bipolar transistor or the n-channel of a 2DEG-FET [2].

The schematic cross-section and the energy band diagram of the 2DEG-HBT are shown in Fig.1 (a) and (b). The outstanding properties [1] of the 2DEG-HBT are summarized as follows:

1. Enhanced bipolar performance due to
 - (a) negligible base transit time of holes due to thin ($\sim 10 \text{ nm}$) 2DEG base without neutral region,
 - (b) very low base resistance r_{bb} ' due to high electron mobility, especially at low temperature (77 K),
2. natural monolithic integration of 2DEG-FET and Pnp-HBT,
3. bifunctional operation of Bipolar/FET as 4 terminal devices.

However, these discussions were based on a simple analytical modeling of 2DEG-HBTs. In this contribution the above advantage will be clearly

demonstrated by using the two-dimensional simulator for heterostructure devices [3], which has been successfully applied to the device analysis of HEMTs [4]. We also demonstrate that it operates simultaneously as a high-performance Pnp HBT and a junction gate 2DEG-FET by the same device structure.

Finally we comment on the bifunctional operation, i.e. the simultaneous bipolar and FET actions. We also report on the present status of the device fabrication.

II. Two-dimensional Numerical Simulation

A. Simulated device structures

The 2DEG-HBT structure modeled in this work is shown in Fig.2. In this work, one of the main concerns is the bipolar/FET characteristics by the same structure so that the source electrode and the drain electrode act also as the two base electrodes. The simulated emitter (gate) size is fixed at $1 \mu\text{m} \times 10 \mu\text{m}$. We have defined the 'central value' of material parameters for the simulated 2DEG-HBT structure, as specified in Table I.

For the sake of comparison, the reference Pnp

HBT is described with the help of Fig.2 and Table I; the intrinsic base is n-GaAs (30 nm, $3 \times 10^{18} \text{ cm}^{-3}$) and the lightly doped collector consists of layer VI (40 nm, 10^{16} cm^{-3}) and layer VII (400 nm, 10^{16} cm^{-3}). The other device parameters are the same with the central values. To clarify the role of the extrinsic base-collector capacitance C_{bc}^{EXT} , an embedded SiO_2 structure is defined by replacing the extrinsic part of the collector layers VII-VIII (Fig.2) by SiO_2 .

B. Device characteristics

The current gain h_{FE} versus collector current density J_C with the life time τ as a parameter is shown in Fig. 3, in which the hole and electron lifetimes were assumed to be equal ($\tau = 1 \text{ ns}$) for SRH type recombination. The collector and base currents' ideality factors are 1.1 and 1.7, respectively. Therefore electron-hole recombination, rather than electron injection into the emitter, dominates the base current of Pnp (2DEG-)HBTs. To confirm the importance of the recombination, the 2DEG-HBT characteristics were also computed with an artificially long carrier lifetime ($\tau = 10^9 \text{ s}$) in all layers.

The carrier concentration profiles are shown in Fig. 4 for the same collector current density. In contrast with the Pnp HBT, the 2DEG-HBT has no neutral base and the metallurgical base region is completely depleted of carriers.

Figure 5 plots the cutoff frequency f_T against the collector current density J_C for the 2DEG-HBT and the Pnp HBT. The maximum cutoff frequencies are 88 GHz at $J_C = 4 \times 10^4 \text{ A/cm}^2$ for the 2DEG-HBT, and 160 GHz for the 2DEG-HBT with the embedded SiO_2 structure.

The 2DEG-HBT achieves its minimum delay time at the high current density of $4 \times 10^4 \text{ A/cm}^2$. In this case, the 1.8 ps computed delay time in Fig. 5 consists of the intrinsic base-emitter delay time $\tau_{be}^{int} (= 0.3 \text{ ps})$, the intrinsic base-collector delay time $\tau_{bc}^{int} (= 0.75 \text{ ps})$, and the extrinsic delay time $\tau^{ext} (= 0.75 \text{ ps})$.

The cutoff frequency f_T is determined mainly

by the collector transit time of holes and the charging time of the extrinsic base-collector capacitance C_{bc}^{EXT} .

From a simple estimation of the base resistance $r_{bb'}$ as $20 \text{ } \Omega$, the maximum oscillation frequency f_{max} can be estimated to be 103 GHz for the SiO_2 embedded structure.

C. Influence of the device parameters

We show one of the examples of the h_{FE} - J_C characteristics of the bipolar mode with the n-AlGaAs doping level N_B as a parameter in Fig.6. At low doping levels, the h_{FE} appears to be as high as 10^5 for a small emitter-base forward bias. This phenomenon is accompanied by a large collector current showing an ideality factor of around 15. In this condition the device could be described as a punch-through diode. The low doping limit of the metallurgical base, n-AlGaAs, is similar to that of devices such as the Bipolar Inversion Channel FET (BICFET) [5,6] or the Inversion Base Transistor (IBT) [7].

D. Bifunctional operations of 2DEG-HBTs

One of the examples of the FET characteristics of the 2DEG-HBT such as the transconductance G_m , the source-drain saturation current I_{DSS} , and the cutoff frequency f_T are shown in Fig. 7 (a) and (b) with the n-AlGaAs doping level N_B as a parameter.

For a large applied gate voltage ($V_G \geq 1.9 \text{ V}$) on the FET characteristics for the embedded SiO_2 structure, the G_m reaches a plateau of 2.4 S/mm shown in Fig. 8 (a). In this region, the source supplies additional electrons to electrically neutralize the large number of holes injected into the heterointerface. The carrier concentration profiles for $V_G = 2 \text{ V}$ explain this situation in Fig. 8 (b).

The bifunction operation, biasing the drain with respect to the source, enables injection of electrons into the channel in excess of the equilibrium 2DEG density. In this case, the maximum cutoff frequency f_T is 225 GHz for collec-

tor current densities of 2×10^4 to 10^5 A/cm², instead of 160 GHz for the bipolar mode.

III. Discussions and Conclusions

This study has demonstrated the device concept and the bipolar/FET operation of the 2DEG-HBT. However, the present status of the device fabrication is still primitive. The example of Gummel plot for the base current I_b (*) and the collector current I_c (o) is shown in Fig. 9. The current gain h_{FE} is 200 for the emitter size of $50 \times 50 \mu\text{m}^2$ at the collector current density $J_c = 4 \times 10^2$ A/cm². The large parasitic resistance between the base and the collector (emitter) prevents the large current density.

However, as the 2DEG-HBT can achieve monolithic integration of PNP HBT and 2DEG-FET by the same epitaxial layer structures, this merged structures of 2DEG-HBT are promising for future high-speed and low-power BiCMOS-like GaAs LSIs.

Acknowledgements

The authors wish to express their gratitude to Dr. H. Matsumura for his continuing encouragements.

References:

- [1] T. Usagawa et al., IEEE IEDM Tech. Dig., pp. 78-81, Dec. 1987.
- [2] T. Mimura et al., Jap. J. Appl. Phys., Vol. 19, pp. L225-L227, 1980.
- [3] T. Ohtoshi et al., Solid St. Electron., Vol. 21, pp. 627-638, 1987.
- [4] H. Mizuta et al., IEEE Trans. Electron Devices, Vol. 36, pp. 2307-2314, 1989.
- [5] G. W. Taylor and J. G. Simmons, IEEE Trans. Electron Devices, Vol. ED-32, pp. 2345-2367, 1985.
- [6] M. Meyyappan et al., Solid-St. Electron., Vol. 26, pp. 1023-1030, 1988.
- [7] K. Matsumoto et al., Extended Abstracts on the 20th conference on Solid State Devices and Materials, pp. 531-534, 1988.

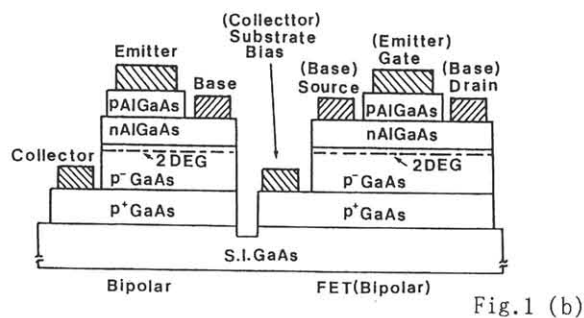


Fig. 1 (b)

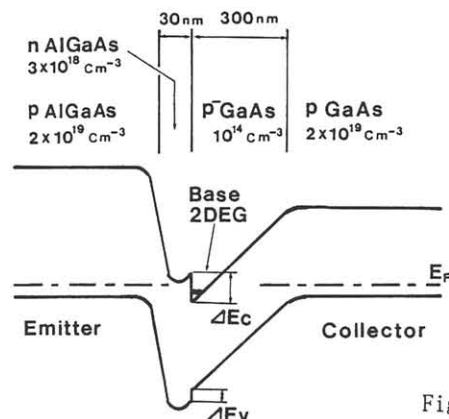


Fig. 1 (a)

Fig. 1 The schematic 2DEG-HBT structure.

- (a) Energy band diagram,
- (b) Cross-sectional view and the natural integration of PNP HBT and 2DEG-FET.

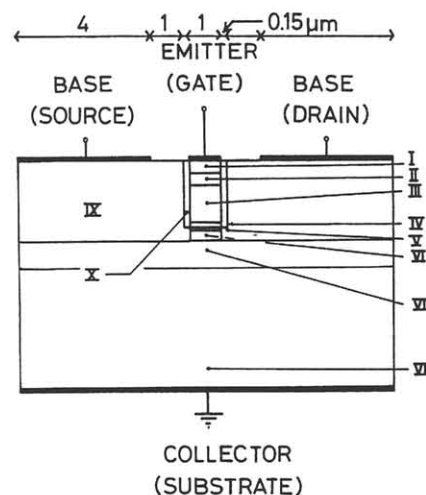


Fig. 2 The simulated 2DEG-HBT structure. The layer structure is described in Table I.

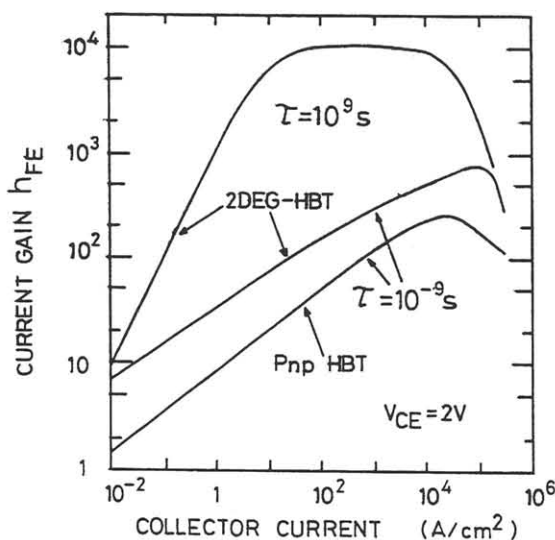


Fig. 3 Common emitter current gain h_{FE} versus collector current density, with the carrier life time as a parameter.

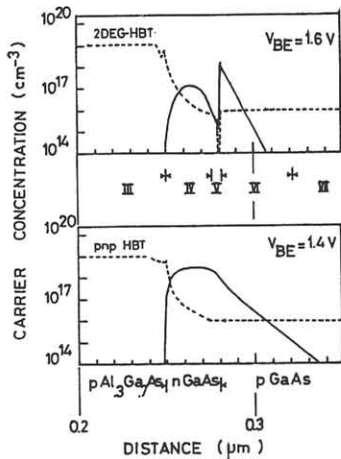


Fig. 4 Electron (solid line) and hole (dashed line) concentration profiles versus distance from the surface in the vicinity of the base, for a collector current density of 10^5 A/cm².

Table I

Layer	Material	Al Fraction	Thickness (nm)	Doping Density (cm ⁻³)
I	p-GaAs		50	10^{20}
I	p-GaAs		50	$5 \cdot 10^{19}$
E	II p-AlGaAs	$X_E = 0.45$	150	$N_E = 10^{19}$
B	IV n-AlGaAs	$X_B = 0.3$	25	$N_B = 2 \cdot 10^{18}$
V	p-AlGaAs	$X_B = 0.3$	6	10^{14}
VI	p-GaAs		$W_C = \begin{cases} 40 \\ 110 \\ 490 \end{cases}$	10^{14}
C	VII p-GaAs			10^{14}
VIII	p-GaAs			10^{19}
IX	n-GaAs			$3 \cdot 10^{18}$
X	SiO ₂			

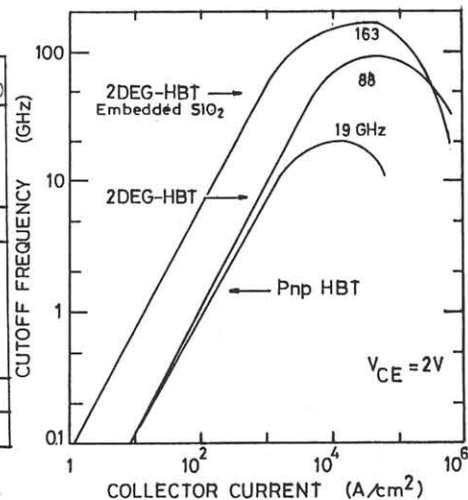


Fig. 5 Cutoff frequency f_T versus collector current density J_C for the Pnp HBT, the 2DEG-HBT and the embedded SiO₂ structure of the 2DEG-HBT.

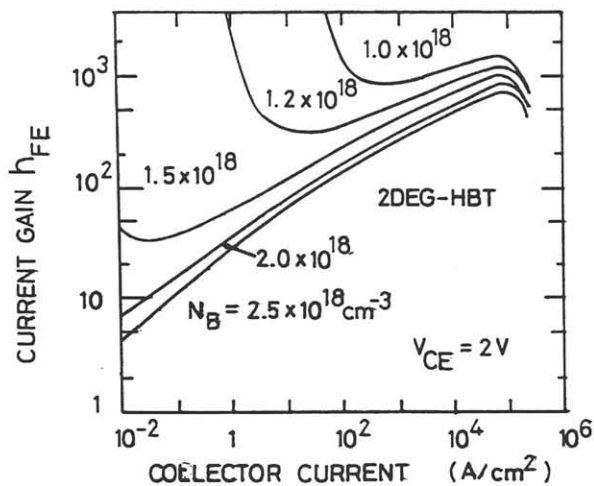


Fig. 6 h_{FE} - J_C characteristics of the 2DEG-HBT with the n-AlGaAs (layer IV) doping level N_B as a parameter.

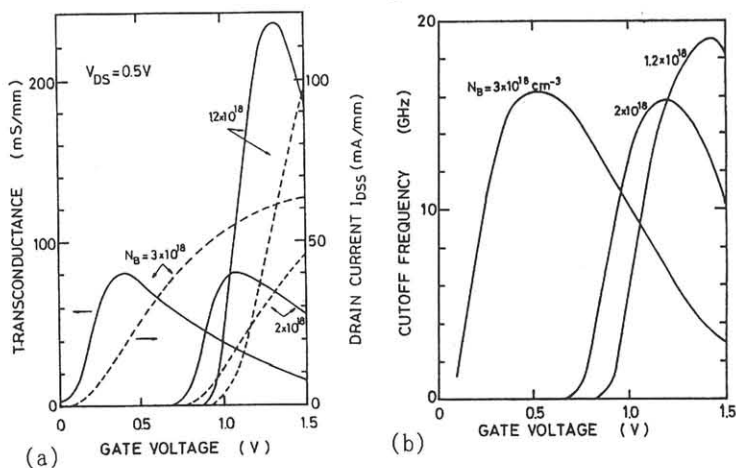


Fig. 7 FET characteristics of the 2DEG-HBT with the n-AlGaAs doping level N_B as a parameter: (a) transconductance (solid line) and drain saturation current (dashed line) versus gate voltage. (b) cutoff frequency versus gate voltage.

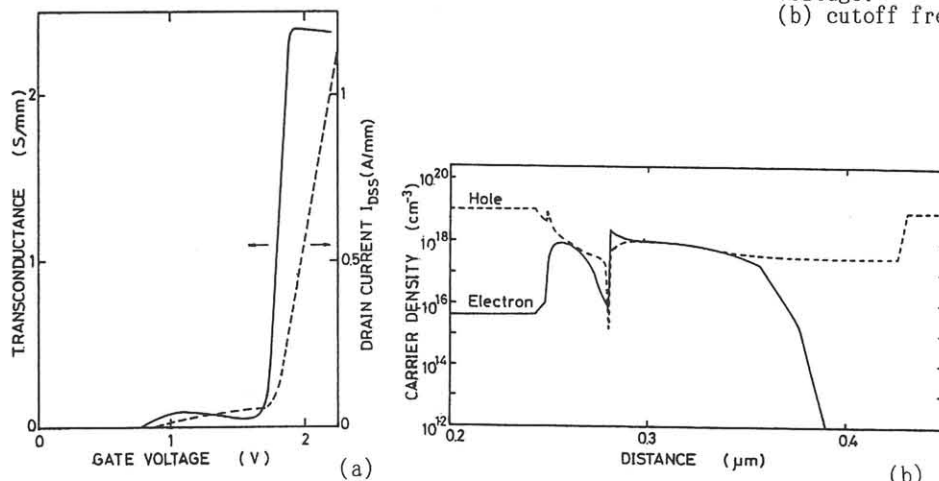


Fig. 8 FET interpretation of the bifunctional mode: (a) transconductance (solid line) and drain saturation current (dashed line) versus gate voltage. (b) Electron (solid line) and hole (dashed line) concentration profiles versus distance from the mid-gate area near the base, for $V_G = 2$ V and a collector current density of 5×10^5 A/cm².

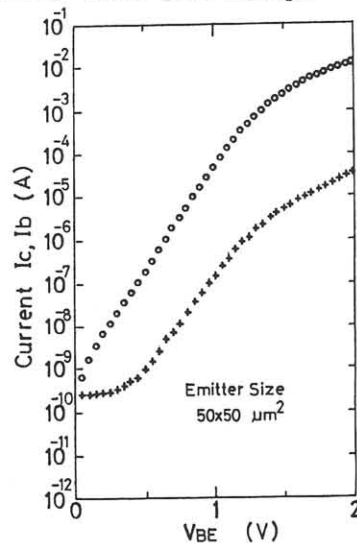


Fig. 9 Gummel plot of the collector current I_C and the base current I_B for the fabricated 2DEG-HBT with the emitter size of $50 \times 50 \mu\text{m}^2$.